



BRIDGE THE GAP BETWEEN THE LORENZ SYSTEM AND THE CHEN SYSTEM

JINHU LÜ*

*Institute of Systems Science
Academy of Mathematics and System Sciences
Chinese Academy of Sciences, Beijing 100080, P.R. China
lvjinhu@amss.ac.cn*

GUANRONG CHEN†

*Department of Electronic Engineering
City University of Hong Kong, Kowloon, Hong Kong, P.R. China*

DAIZHAN CHENG

*Institute of Systems Science
Academy of Mathematics and System Sciences
Chinese Academy of Sciences, Beijing 100080, P.R. China*

SERGEJ CELIKOVSKY‡

*Institute of Information Theory and Automation
Academy of Sciences of the Czech Republic
P.O. Box 12, 182 08 Prague 8, Czech Republic*

Received September 12, 2001; Revised November 1, 2001

This paper introduces a unified chaotic system that contains the Lorenz and the Chen systems as two dual systems at the two extremes of its parameter spectrum. The new system represents the continued transition from the Lorenz to the Chen system and is chaotic over the entire spectrum of the key system parameter. Dynamical behaviors of the unified system are investigated in somewhat detail.

Keywords: Lorenz system; Chen system; critical system; a unified chaotic system.

1. Introduction

Recently, the study of chaotic dynamics has evolved from the traditional trend of understanding and analyzing chaos to the new intention of controlling and utilizing it [Chen & Dong, 1998; Wang & Chen, 2000; Lü *et al.*, 2002d].

The Lorenz system, found in 1963, produces the best-known canonical chaotic attractor in a sim-

ple three-dimensional autonomous system [Lorenz, 1963; Stewart, 2000]. In 1999, Chen found a similar but nonequivalent chaotic attractor [Chen & Ueta, 1999; Ueta & Chen, 2000], which is now known to be the *dual* of the Lorenz system, in a sense defined in [Vaněček & Čelikovský, 1996]: The Lorenz system satisfies the condition $a_{12}a_{21} > 0$ while the Chen system satisfies $a_{12}a_{21} < 0$. Very recently, Lü and Chen [2002] reported a new chaotic

*Author for correspondence.

†Supported by the Hong Kong Research Grants Council under the CERG Grant no. 9040579.

‡Supported by the Grant Agency of CR through the grant no. 102/99/1368.

system, which satisfies the condition $a_{12}a_{21} = 0$, called Lü system by others [Yu & Zhang, 2003], thereby bridging the gap between the Lorenz and the Chen systems.

It is notable that the above three systems share some common properties: (1) they all have the same symmetry, dissipativity, stability of equilibria, and similar bifurcations and topological structures, etc. In fact, they belong to the generalized Lorenz canonical family [Čelikovský & Chen, 2002]. (2) They have a compound structure [Lü *et al.*, 2002b; Lü *et al.*, 2002c]. (3) The familiar Duffing oscillator can be controlled to both the Lorenz and the Chen systems [Kunin & Chen, 1997; Čelikovský & Chen, 2002].

We have pointed out [Lü & Chen, 2002; Lü *et al.*, 2002a] that the new chaotic system found in [Lü & Chen, 2002] is a transition system between the Lorenz and the Chen systems. It is therefore interesting to ask if there is a chaotic system that can unify the aforementioned three chaotic systems, and can realize the continued transition from one to another. This paper provides a positive answer to this question.

2. The Unified System

Based on the concept of generalized Lorenz system [Vaněček & Čelikovský, 1996], Čelikovský and Chen [2002] introduced the broader generalized Lorenz canonical form. Notice, however, that although the generalized Lorenz canonical form contains both the Lorenz and the Chen systems, their relationship and particularly the transition between them are not very transparent. Here, we introduce a unified system that not only bridges the gap between the Lorenz and the Chen system but also represent the entire family of chaotic systems between them. To that end, the dynamical behaviors of this family of chaotic systems will be investigated.

The new unified system is described by

$$\begin{cases} \dot{x} = (25\alpha + 10)(y - x) \\ \dot{y} = (28 - 35\alpha)x - xz + (29\alpha - 1)y \\ \dot{z} = xy - \frac{\alpha + 8}{3}z, \end{cases} \quad (1)$$

where $\alpha \in [0, 1]$.

According to [Vaněček & Čelikovský, 1996], the linear part of system (1), a constant matrix $A = [a_{ij}]_{3 \times 3}$, provides a critical value $a_{12}a_{21}$.

According to this critical value, the whole family of chaotic systems (1) can be classified as follows: when $0 \leq \alpha < 0.8$, system (1) belongs to the generalized Lorenz system defined in [Vaněček & Čelikovský, 1996], since with these values of α in the above equation one has $a_{12}a_{21} > 0$; when $\alpha = 0.8$, it belongs to the class of chaotic systems introduced in [Lü & Chen, 2002; Lü *et al.*, 2002a], since in this case $a_{12}a_{21} = 0$; when $0.8 < \alpha \leq 1$, it belongs to the generalized Chen system formulated in [Čelikovský & Chen, 2002], for which $a_{12}a_{21} < 0$.

Simulations and numerical analysis suggest that the Chen attractor has many different and yet more complicated topological structures and properties as compared to the Lorenz attractor [Ueta & Chen, 2000]. When the parameter α increases from 0 to 1, system (1) evolves from the Lorenz attractor to the Chen attractor, which will be further discussed below.

Here, some special features and advantages of system (1) are first summarized:

- (i) System (1) is a chaotic system when $\alpha \in [0, 1]$;
- (ii) System (1) is very simple and has only one key parameter α . One can use the so-called complementary-cluster energy-barrier criterion (CCEBC) to analyze this system [Xue, 1999];
- (iii) System (1) connects the Lorenz and the Chen systems, and realizes the entire transition spectrum from one to the other;
- (iv) The control of the parameter α in system (1) reveals the evolution of dynamical behaviors from Lorenz attractor to Chen attractor;
- (v) The periodic windows of system (1) reveal the true reason as to why the Lorenz and the Chen attractors have similar but different topological structures.

3. Dynamical Behaviors of the Unified System

3.1. Some basic properties

System (1) shares several important qualitative properties with both the Lorenz and the Chen systems. This is further discussed in the following.

(1) Symmetry and invariance

The Lorenz and the Chen systems both have a natural symmetry under the coordinates transform $(x, y, z) \rightarrow (-x, -y, z)$. Similarly, it is easy to verify the invariance of system (1) under the same

transformation, i.e. the reflection about the z -axis. The symmetry persists for all values of the system parameters $\alpha \in [0, 1]$. Also, it is clear that the z -axis itself is an orbit (an invariant manifold), i.e. if $x = y = 0$ at $t = t_0$ then $x = y = 0$ for all $t \geq t_0$. Furthermore, the trajectory on the z -axis tends to the origin as $t \rightarrow \infty$, since for such a trajectory, $\frac{dx}{dt} = \frac{dy}{dt} = 0$ and $\frac{dz}{dt} = -\frac{\alpha+8}{3}z$. Therefore, system (1) shares the symmetry and invariance with both the Lorenz and Chen systems for all values of α .

(2) Dissipativity and the existence of attractor

For system (1), one has

$$\nabla V = \frac{\partial \dot{x}}{\partial x} + \frac{\partial \dot{y}}{\partial y} + \frac{\partial \dot{z}}{\partial z} = -\frac{41 - 11\alpha}{3}.$$

Hence, for all $\alpha \in [0, 1]$, which satisfy $41 - 11\alpha > 0$, system (1) is dissipative, with an exponential contraction rate:

$$\frac{dV}{dt} = e^{-\frac{41-11\alpha}{3}t}.$$

That is, a volume element V_0 is contracted by the flow into a volume element $V_0 e^{-\frac{41-11\alpha}{3}t}$ in time t . This means that each volume containing the system trajectory shrinks to zero as $t \rightarrow \infty$ at an exponential rate $-\frac{41-11\alpha}{3}$. In fact, numerical simulations have shown that system orbits are ultimately confined into a specific limit set of zero volume, and the system asymptotic motion settles onto an attractor. Thus, system (1) has the same dissipativity as both the Lorenz and Chen systems for any value of $\alpha \in [0, 1]$.

3.2. Equilibria and stability

The equilibria of system (1) can be easily found by solving the three equations $\dot{x} = \dot{y} = \dot{z} = 0$, which lead to

$$\begin{aligned} (25\alpha + 10)(y - x) &= 0, \\ (28 - 35\alpha)x - xz + (29\alpha - 1)y &= 0, \end{aligned}$$

and

$$xy - \frac{\alpha + 8}{3}z = 0.$$

It can be easily verified that there are three equilibria:

$$\begin{aligned} &S_0(0, 0, 0) \\ S_- &(-\sqrt{(8 + \alpha)(9 - 2\alpha)}, -\sqrt{(8 + \alpha)(9 - 2\alpha)}, 27 - 6\alpha) \\ S_+ &(\sqrt{(8 + \alpha)(9 - 2\alpha)}, \sqrt{(8 + \alpha)(9 - 2\alpha)}, 27 - 6\alpha), \end{aligned}$$

in which two equilibria, S_- and S_+ , are symmetrically placed with respect to the z -axis.

Linearizing the unified system (1) about the equilibrium S_0 provides an eigenvalue $\lambda_1 = -\frac{\alpha+8}{3}$ along with the following characteristic equation:

$$\begin{aligned} f(\lambda) &= \lambda^2 + (11 - 4\alpha)\lambda \\ &+ (25\alpha + 10)(6\alpha - 27) = 0. \end{aligned} \tag{2}$$

Since $\alpha \in [0, 1]$, it always satisfies both $11 - 4\alpha > 0$ and $(25\alpha + 10)(6\alpha - 27) < 0$, and the two eigenvalues satisfy $\lambda_2 > 0 > \lambda_3$. So, the equilibrium S_0 is a saddle point in the three-dimensional phase space.

Next, linearizing the system about the other equilibria yields the following characteristic equation:

$$\begin{aligned} f(\lambda) &= \lambda^3 + \frac{41 - 11\alpha}{3}\lambda^2 \\ &+ \frac{(38 - 10\alpha)(\alpha + 8)}{3}\lambda \\ &+ 2(25\alpha + 10)(\alpha + 8)(9 - 2\alpha) = 0. \end{aligned} \tag{3}$$

Obviously, the two equilibria S_{\pm} have the same stability characterization. Let

$$\begin{aligned} A &= \frac{41 - 11\alpha}{3} \\ B &= \frac{(38 - 10\alpha)(\alpha + 8)}{3} \\ C &= 2(25\alpha + 10)(\alpha + 8)(9 - 2\alpha). \end{aligned} \tag{4}$$

The Routh–Hurwitz conditions lead to the conclusion that the real parts of the roots λ are negative if and only if

$$\frac{41 - 11\alpha}{3} > 0, \quad 2(25\alpha + 10)(\alpha + 8)(9 - 2\alpha) > 0,$$

and

$$\frac{2(\alpha + 8)(505\alpha^2 - 2259\alpha - 31)}{9} > 0,$$

namely, if and only if $\alpha < -0.0137$. But this is impossible for $\alpha \in [0, 1]$.

Note that the coefficients of the cubic polynomial (3) are all positive. Therefore, $f(\lambda) > 0$ for all $\lambda > 0$. Consequently, there is instability ($\text{Re}(\lambda) > 0$) only if there are two complex conjugate

zeros of f . Let the two complex zeros be $\lambda_1 = i\omega$ and $\lambda_2 = -i\omega$ for some real ω . Note that the sum of the three zeros of the cubic f is

$$\lambda_1 + \lambda_2 + \lambda_3 = -\frac{41 - 11\alpha}{3}.$$

Hence, $\lambda_3 = -\frac{41-11\alpha}{3}$, on the margin of stability, where $\lambda_{1,2} = \pm i\omega$. On this margin,

$$\begin{aligned} 0 &= f\left(-\frac{41 - 11\alpha}{3}\right) \\ &= \frac{2(\alpha + 8)(-505\alpha^2 + 2259\alpha + 31)}{9}, \end{aligned}$$

that is,

$$\alpha_{1,2} = \frac{2259 \pm \sqrt{5165701}}{1010}.$$

Since

$$-0.0137 < 0 \leq \alpha \leq 1 < 4.4869,$$

the two equilibria S_{\pm} are unstable.

Actually, one can determine the exact values of the eigenvalues by setting $\lambda = -\frac{A}{3} + \Lambda$ in (3). This yields

$$f(\Lambda) = \Lambda^3 + P\Lambda + Q,$$

where $P = -\frac{A^2}{3} + B$ and $Q = \frac{2A^3}{27} - \frac{AB}{3} + C$. This third-order polynomial in Λ can be solved by using the Cardan formula, whereby one may set $\Delta = 4P^3 + 27Q^2$. Since

$$P = \frac{-211\alpha^2 + 524\alpha + 1055}{27} > 0 \text{ for } \alpha \in [0, 1],$$

one has

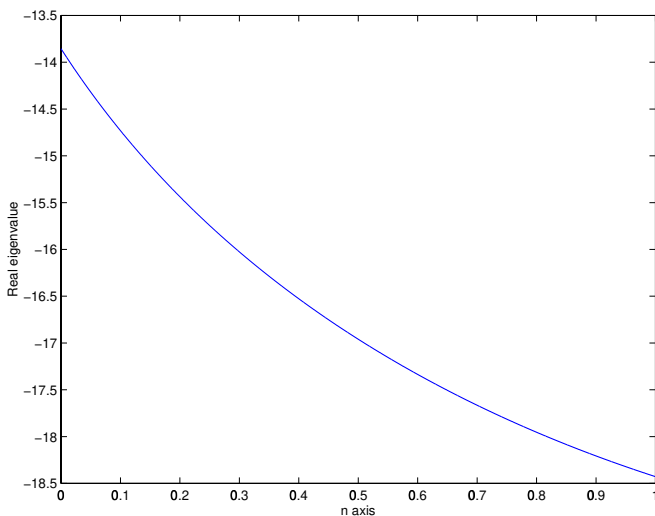
$$\Delta = 4P^3 + 27Q^2 > 0.$$

Therefore, Eq. (3) has a unique real eigenvalue:

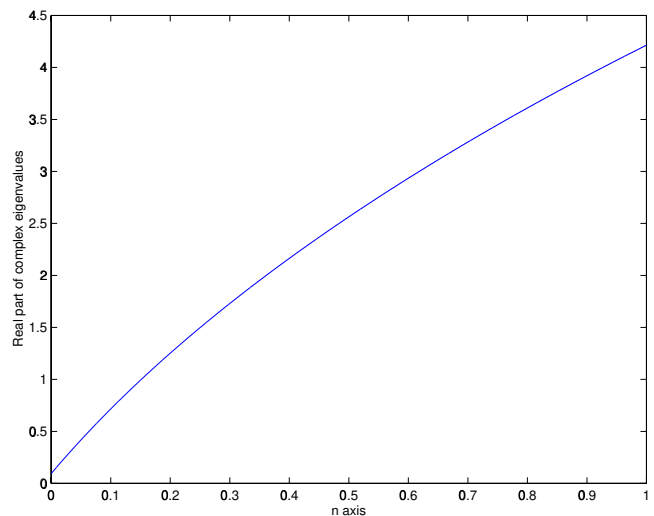
$$\begin{aligned} \lambda_R &= -\frac{A}{3} + \Lambda_R \\ &= -\frac{A}{3} + \frac{1}{6} \sqrt[3]{-108Q + 12\sqrt{12P^3 + 81Q^2}} \\ &\quad - \frac{2P}{\sqrt[3]{-108Q + 12\sqrt{12P^3 + 81Q^2}}}, \end{aligned} \tag{5}$$

along with two complex conjugate eigenvalues:

$$\begin{aligned} (\lambda_C)_{\pm} &= -\frac{A}{3} + (\Lambda_C)_{\pm} \\ &= -\frac{A}{3} - \frac{1}{12} \sqrt[3]{-108Q + 12\sqrt{12P^3 + 81Q^2}} \\ &\quad + \frac{P}{\sqrt[3]{-108Q + 12\sqrt{12P^3 + 81Q^2}}} \\ &\quad \pm \frac{\sqrt{3}}{2} i \left(\frac{1}{6} \sqrt[3]{-108Q + 12\sqrt{12P^3 + 81Q^2}} \right. \\ &\quad \left. + \frac{2P}{\sqrt[3]{-108Q + 12\sqrt{12P^3 + 81Q^2}}} \right). \end{aligned} \tag{6}$$



(a)



(b)

Fig. 1. (a) The real eigenvalue $\lambda_R(\alpha)$; (b) the real part of complex conjugate eigenvalues $-\frac{A}{3} - \frac{\Lambda_R}{2}$.

By some tedious manipulations, one can get the exact algebraic expression of α for a unique real eigenvalue $\lambda_R(\alpha)$. And the correlation between α and $\lambda_R(\alpha)$ is shown in Fig. 1(a). According to Fig. 1(a), one can see that $\lambda_R(\alpha)$ is a decreasing function of α and $\lambda_R(\alpha) < 0$ for all $\alpha \in [0, 1]$. Similarly, the correlation between α and the real part of the complex conjugate eigenvalues $-\frac{A}{3} - \frac{\Lambda_R}{2}$ is shown in Fig. 1(b). Figure 1(b) shows that $-\frac{A}{3} - \frac{\Lambda_R}{2}$ is an increasing function of α and $-\frac{A}{3} - \frac{\Lambda_R}{2} > 0$ for all $\alpha \in [0, 1]$. Therefore, the two equilibria S_{\pm} of system (1) are always unstable for all $\alpha \in [0, 1]$. That is, the three equilibria of system (1) are unstable for all $\alpha \in [0, 1]$.

3.3. Dynamical analysis of the new system

In the following, we will use the complementary-cluster energy-barrier criterion (CCEBC) [Xue, 1999] to investigate the dynamical behaviors of the unified system (1).

First, consider the first and second equations of the system:

$$\begin{cases} \dot{x} = (25\alpha + 10)(y - x), \\ \dot{y} = (28 - 35\alpha - z)x + (29\alpha - 1)y, \end{cases} \quad (7)$$

where $\alpha \in [0, 1]$, x, y are status variables and z is considered as a known function of time variable t .

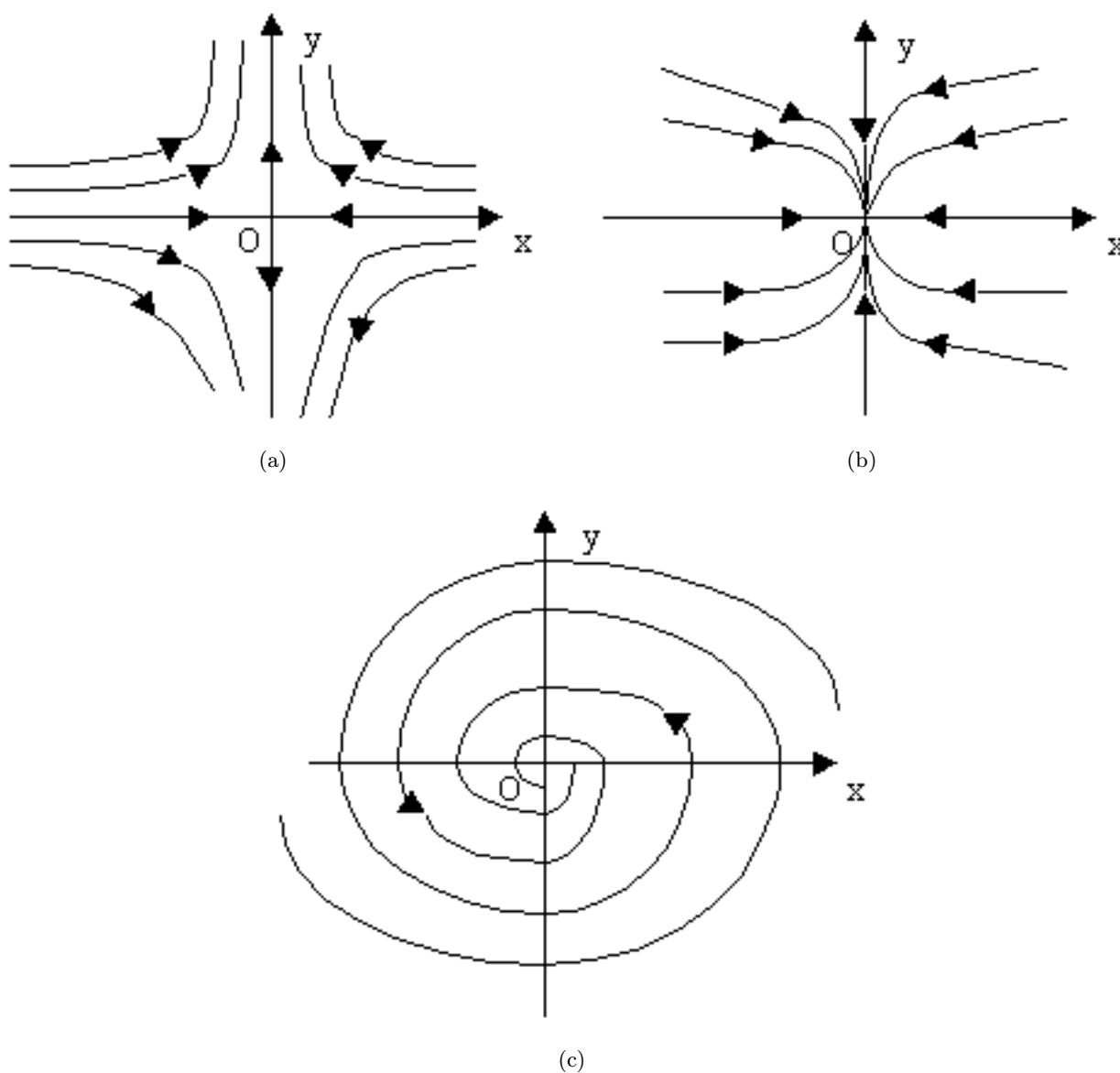


Fig. 2. The solution curve of system (8). (a) $z < 27 - 6\alpha$; (b) $27 - 6\alpha < z < 27 - 6\alpha + \frac{(11-4\alpha)^2}{20(5\alpha+2)}$; (c) $z > 27 - 6\alpha + \frac{(11-4\alpha)^2}{20(5\alpha+2)}$.

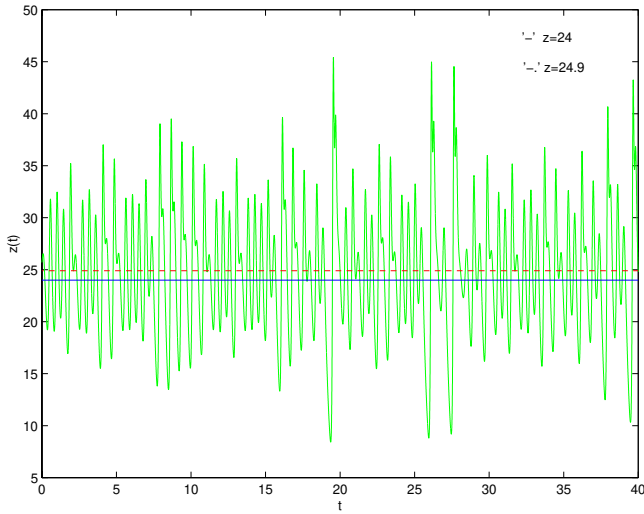


Fig. 3. The time series of $z(t)$.

In particular, when z is a constant independent of x , y and t , system (7) can be regarded as a two-dimensional linear system with constant coefficients. In this trivial case, its dynamical behavior is very simple and global. Especially, when this constant $z \neq 27 - 6\alpha$, the origin $(0, 0)$ is the only equilibrium of system (7). Linearizing system (1) about the equilibrium $(0, 0)$ gives the following characteristic equation:

$$f(\lambda) = \lambda^2 + (11 - 4\alpha)\lambda + (25\alpha + 10)(6\alpha - 27 + z) = 0. \quad (8)$$

- (1) For $0 \leq \alpha \leq 1$, when $z < 27 - 6\alpha$, the two eigenvalues satisfy $\lambda_1 > 0 > \lambda_2$, so the equilibrium $(0, 0)$ is a saddle point in the two-dimensional plane. The solution curve in the x - y plane is shown in Fig. 2(a), where the direction of arrow is the direction of the orbit as t increases. When t goes to infinity, only two orbits go to the origin, and the other orbits go to infinity along two different directions.
- (2) When $27 - 6\alpha < z < 27 - 6\alpha + \frac{(11-4\alpha)^2}{20(5\alpha+2)}$, Eq. (8) has two different negative real roots. The equilibrium $(0, 0)$ is a node. The solution curve in the x - y plane is shown in Fig. 2(b), where the direction of arrow is the direction of the orbit as t increases. When t goes to infinity, all but two orbits go to infinity along two different directions.
- (3) When $z > 27 - 6\alpha + \frac{(11-4\alpha)^2}{20(5\alpha+2)}$, Eq. (8) has two complex conjugate eigenvalues with a negative real part. The equilibrium $(0, 0)$ is a focus.

The solution curve in the x - y plane is shown in Fig. 2(c), where the direction of arrow is the direction of the orbit as t increases. When t goes to infinity, all orbits spiral into the origin.

Now, we take a closer look at the dynamical behaviors of the unified system (1). In all the simulations here, for any chosen initial condition $x(0) = x_0$, $y(0) = y_0$, $z(0) = z_0$, the time step size $h = 0.001$, parameter $\alpha = 0.5$, and the time series $x(t)$, $y(t)$, $z(t)$ are generated by the fourth-order Runge–Kutta algorithm. Figure 3 shows the correlation between the time variable t and the function $z(t)$.

It can be seen that when $t \rightarrow \infty$, the orbit $z(t)$ goes through the straight lines $z = 27 - 6\alpha$ and $z = 27 - 6\alpha + \frac{(11-4\alpha)^2}{20(5\alpha+2)}$ alternatively, and repeatedly many times. The z -axis is partitioned into three disjoint domains: $(-\infty, 27 - 6\alpha)$, $(27 - 6\alpha, 27 - 6\alpha + \frac{(11-4\alpha)^2}{20(5\alpha+2)})$, and $(27 - 6\alpha + \frac{(11-4\alpha)^2}{20(5\alpha+2)}, +\infty)$, by the two straight lines $z = 27 - 6\alpha$ and $z = 27 - 6\alpha + \frac{(11-4\alpha)^2}{20(5\alpha+2)}$.

System (7) has different dynamical behaviors in the above three different domains. When $t \rightarrow \infty$, system (1) changes dynamical behaviors when $z(t)$ goes through these domains repeatedly. That is, the dynamical behaviors of system (1) is changing repeatedly, leading to complex dynamics such as the appearance of bifurcations and chaos.

4. Controlling the Duffing Oscillator to the Unified System

The familiar Duffing oscillator can be controlled to the canonical Lorenz and Chen systems [Kunin & Chen, 1997; Čelikovský & Chen, 2002]. Here, a similar connection between the Duffing oscillator and the unified system (1) can be found.

Theorem 1. The controlled Duffing oscillator

$$\frac{d^2 x_d}{dt^2} + \mu \frac{dx_d}{dt} + (\varepsilon x_d^2 - 1)x_d = -u x_d, \quad (9)$$

with parameter $\mu = 11 - 4\alpha$ and the dynamical feedback controller u satisfying

$$\begin{aligned} \frac{du}{dt} = & \lambda_3 u + \varepsilon(\lambda_3 + 50\alpha + 20)x_d^2 \\ & - \lambda_3(150\alpha^2 - 615\alpha - 269) \end{aligned} \quad (10)$$

is diffeomorphic to the unified system (1) via the following linear transformation:

$$\begin{aligned} x_d &= \frac{x}{\sqrt{2\varepsilon}}, \\ \frac{dx_d}{dt} &= \frac{(25\alpha + 10)(y - x)}{\sqrt{2\varepsilon}}, \\ u &= (25\alpha + 10)z - \frac{x^2}{2} \end{aligned} \tag{11}$$

Alternatively, system (9) can be transformed into the unified system (1) by using the parameter $\mu = \frac{11-4\alpha}{\sqrt{-150\alpha^2+615\alpha+270}}$ and the dynamical feedback controller

$$\frac{du}{dt} = \frac{\lambda_3 u + \varepsilon(\lambda_3 + 50\alpha + 20)x_d^2}{\sqrt{-150\alpha^2 + 615\alpha + 270}}, \tag{12}$$

with the following linear transformation:

$$\begin{aligned} x_d &= \frac{x}{\sqrt{2\varepsilon(-150\alpha^2 + 615\alpha + 270)}} \\ \frac{dx_d}{dt} &= \frac{(25\alpha + 10)(y - x)}{(-150\alpha^2 + 615\alpha + 270)\sqrt{2\varepsilon}}, \\ u &= \frac{(25\alpha + 10)z - \frac{x^2}{2}}{-150\alpha^2 + 615\alpha + 270}, \end{aligned} \tag{13}$$

and with the following time-rescaling:

$$t = \sqrt{-150\alpha^2 + 615\alpha + 270}\theta, \tag{15}$$

where the time variable in the unified system (1) is denoted as t and that in the Duffing equation as θ .

Proof. Applying to the unified system (1) the coordinate change

$$\begin{aligned} x' &= \frac{x}{\sqrt{-2\varepsilon}}, \\ y' &= \frac{(25\alpha + 10)(y - x)}{\sqrt{-2\varepsilon}}, \\ z' &= (25\alpha + 10)z - \frac{x^2}{2} + 150\alpha^2 - 615\alpha - 269, \end{aligned}$$

after straightforward but somewhat tedious computations, one obtains

$$\begin{cases} \frac{dx'}{dt} = y' \\ \frac{dy'}{dt} = x'(1 - \varepsilon(x')^2) + (4\alpha - 11)y' - x'z' \\ \frac{dz'}{dt} = \lambda_3 z' + \varepsilon(\lambda_3 + 50\alpha + 20)(z')^2 - \lambda_3(150\alpha^2 - 615\alpha - 269). \end{cases} \tag{16}$$

Then, denoting $x_d \equiv x'$ and $u \equiv z'$, and by using the first equation of (16), $\frac{dx_d}{dt} \equiv y'$, the last two equations in (16) are converted exactly into those of (9) and (10), with parameter $\mu = 4\alpha - 11$.

Similarly, the case with time-rescaling can be proved. Applying the coordinate change

$$\begin{aligned} x' &= \frac{x}{\sqrt{2\varepsilon(-150\alpha^2 + 615\alpha + 270)}}, \\ y' &= \frac{(25\alpha + 10)(y - x)}{(-150\alpha^2 + 615\alpha + 270)\sqrt{2\varepsilon}}, \\ z' &= \frac{(25\alpha + 10)z - \frac{x^2}{2}}{-150\alpha^2 + 615\alpha + 270}, \end{aligned}$$

one has

$$\begin{cases} \frac{dx'}{dt} = \sqrt{-150\alpha^2 + 615\alpha + 270}y' \\ \frac{dy'}{dt} = \sqrt{-150\alpha^2 + 615\alpha + 270}x'(1 - \varepsilon(x')^2) + (4\alpha - 11)y' - \sqrt{-150\alpha^2 + 615\alpha + 270}x'z' \\ \frac{dz'}{dt} = \lambda_3 z' + \varepsilon(\lambda_3 + 50\alpha + 20)(x')^2. \end{cases} \tag{17}$$

Under the time rescaling (15) and denoting $x_d \equiv x'$, $\frac{dx_d}{dt} \equiv y'$, $u \equiv z'$, the last two equations of (17) are converted into those of (9) and (12), with $\mu = \frac{4\alpha-11}{\sqrt{-150\alpha^2+615\alpha+270}}$. The proof is thus completed. ■

5. Numerical Simulations

As mentioned, the unified system (1) contains the

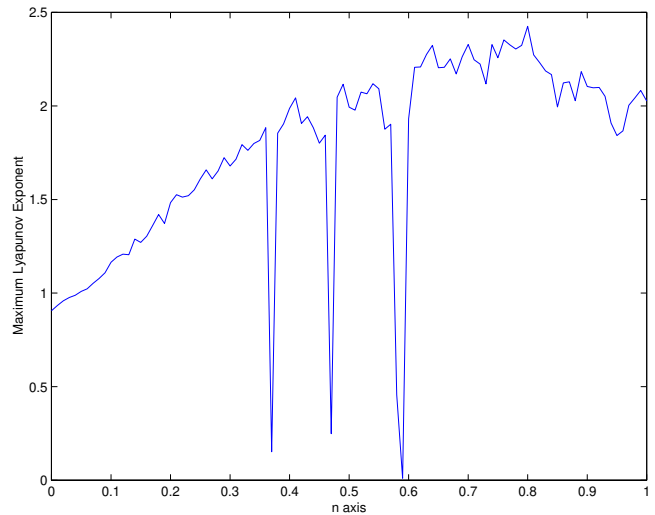


Fig. 4. The maximum Lyapunov exponent of system (1).

canonical Lorenz system [Čelikovský & Chen, 2002], the Chen system [Chen & Ueta, 1999; Ueta & Chen, 2000], and the chaotic system recently introduced in [Lü & Chen, 2002] as special cases.

The maximum Lyapunov exponents of system (1) are shown in Fig. 4, while Figs. 5(a)–5(h) show some snapshots taken from the entire spectrum of the chaotic transition between the two extremes —

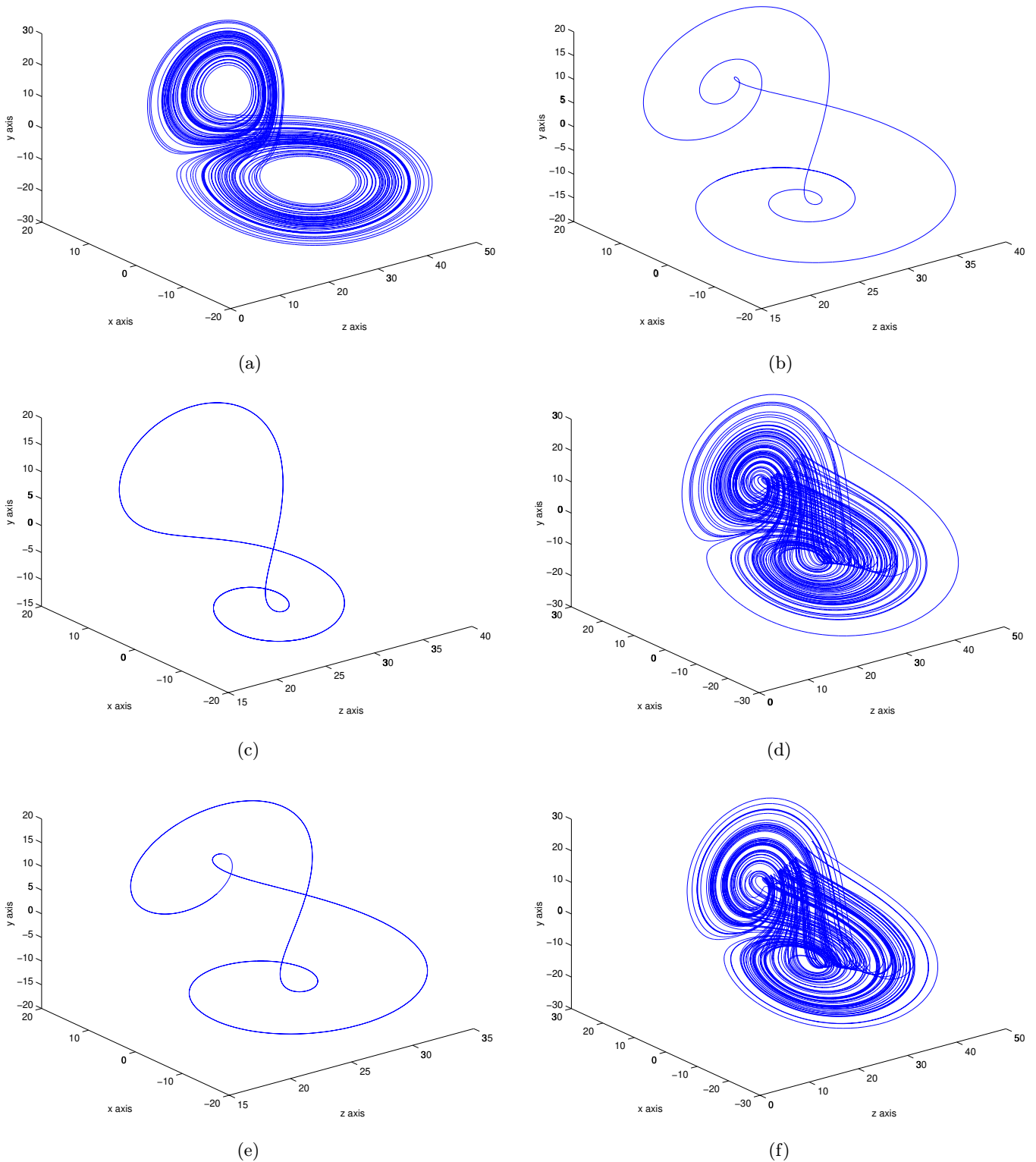


Fig. 5. The phase portraits of system (1). (a) $\alpha = 0$; (b) $\alpha = 0.37$; (c) $\alpha = 0.47$; (d) $\alpha = 0.5$; (e) $\alpha = 0.59$; (f) $\alpha = 0.6$; (g) $\alpha = 0.8$; (h) $\alpha = 1$.

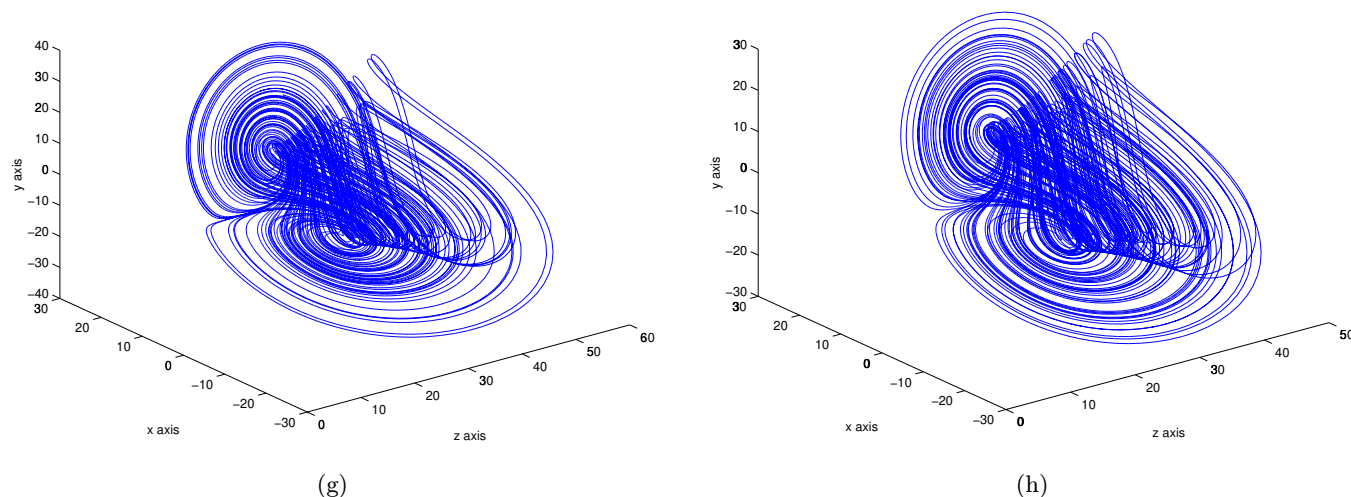


Fig. 5. (Continued)

the Lorenz and the Chen attractors. In these figures, only a single parameter α is tuned: $\alpha \in [0, 1]$. Figure 5(a) is the original Lorenz attractor; Fig. 5(g) is the typical chaotic attractor reported in [Lü & Chen, 2002]; Fig. 5(h) is the original Chen attractor. It is clear that with the increasing of the parameter α , the topological structure of the chaotic attractor becomes more and more complex.

It is noticed that system (1) has three periodic windows: $W_1 = [0.369, 0.371]$, $W_2 = [0.468, 0.470]$, $W_3 = [0.575, 0.597]$. These periodic windows divide the whole interval $[0, 1]$ into four chaotic intervals: $I_1 = [0, 0.36]$, $I_2 = [0.38, 0.46]$, $I_3 = [0.48, 0.57]$ and $I_4 = [0.6, 1]$. When $\alpha \in I_1$, the topological structure of system (1) is similar to the original Lorenz attractor; when $\alpha \in I_2$, this topological structure is a variant of Lorenz attractor; when $\alpha \in I_3$, it is a variant of the Chen attractor; when $\alpha \in I_4$, it becomes similar to the Chen attractor. Figure 5(d) displays the variant of the Chen attractor, and Figs. 5(f) and 5(g) show their similar structures to that of the Chen attractor. Particularly notable is that Fig. 5(g) belongs to the chaotic system discussed in [Lü *et al.*, 2002b]. Figures 5(b), 5(c) and 5(e) display some typical periodic orbits of system (1).

It is very interesting to point out that the Chen attractor can be derived from the periodic orbit shown in Fig. 5(e). Similarly, the Lorenz attractor can be derived from the periodic orbit shown in Fig. 5(b). Even more interesting is that the periodic orbit shown in Fig. 5(c) is the transition between the two periodic orbits shown in Figs. 5(b)

and 5(e), respectively. It is the very reason that the Lorenz and the Chen attractors have similar but different topological structures but they are connected through such a chaotic transition.

6. Conclusions

A unified chaotic system has been introduced and discussed in this paper. The unified system is produced as a kind of unique and unified classification between the Lorenz and the Chen attractors, both in theory and in simulation. In fact, this unified system is likely to be the simplest chaotic system that bridges the gap between the Lorenz and the Chen systems, and contributes to a better understanding of the correlation between the Lorenz attractor and the Chen attractor.

References

- Čelikovský, S. & Chen, G. [2002] "On a generalized Lorenz canonical form of chaotic systems," *Int. J. Bifurcation and Chaos* **12**, 1789–1812.
- Chen, G. & Dong, X. [1998] *From Chaos to Order: Methodologies, Perspectives and Applications* (World Scientific, Singapore).
- Chen, G. & Ueta, T. [1999] "Yet another chaotic attractor," *Int. J. Bifurcation and Chaos* **9**, 1465–1466.
- Kunin, I. & Chen, G. [1997] "Controlling the Duffing oscillator to the Lorenz system and generalization," *Proc. Int. Conf. Control of Oscillations and Chaos*, St. Petersburg, Russia, 27–29 August, 1997, pp. 419–422.
- Lorenz, E. N. [1963] "Deterministic nonperiodic flows," *J. Atmos. Sci.* **20**, 130–141.

- Lü, J. & Chen, G. [2002] “A new chaotic attractor coined,” *Int. J. Bifurcation and Chaos* **12**, 659–661.
- Lü, J., Chen, G. & Zhang, S. [2002a] “Dynamical analysis of a new chaotic attractor,” *Int. J. Bifurcation and Chaos* **12**, 1001–1015.
- Lü, J., Zhou, T., Chen, G. & Zhang, S. [2002b] “The compound structure of Chen’s attractor,” *Int. J. Bifurcation and Chaos* **12**, 855–858.
- Lü, J., Chen, G. & Zhang, S. [2002c] “The compound structure of a new chaotic attractor,” *Chaos Solit. Fract.* **14**, 669–672.
- Lü, J., Lu, J. & Chen, S. [2002d] *Chaotic Time Series Analysis and Its Applications* (Wuhan University Press, Wuhan, China).
- Stewart, I. [2000] “The Lorenz attractor exists,” *Nature* **406**, 948–949.
- Ueta, T. & Chen, G. [2000] “Bifurcation analysis of Chen’s attractor,” *Int. J. Bifurcation and Chaos* **10**, 1917–1931.
- Vaněček, A. & Čelikovský, S. [1996] *Control Systems: From Linear Analysis to Synthesis of Chaos* (Prentice-Hall, London).
- Wang, X. & Chen, G. [2000] “Chaotification via arbitrarily small feedback controls: Theory, method, and applications,” *Int. J. Bifurcation and Chaos* **10**, 549–570.
- Xue, Y. [1999] *Quantitative Study of General Motion Stability and an Example on Power System Stability* (Jiangsu Science and Technology Press, Nanjing, China).
- Yu, Y. & Zhang, S. [2003] “Controlling uncertain Lü system using backstepping design,” *Chaos Solit. Fract.* **15**, 897–902.